NUMERICAL STUDY ON CO_2 ABSORPTION EFFICIENCY BY USING AQUEOUS MONOETHANOLAMINE SOLUTION IN CO_2 ABSORBER COLUMN

Sung-Min Shim[a], Sang-Jin Lee[b], Jung-Gil Lee[a] and Woo-Seung Kim[c*]
[a]Department of Mechanical Engineering, Hanyang University, 17 Haengdang-dong, Seongdong-gu, Seoul, Republic of Korea
[b]STX Heavy Industries Co., Ltd, Environment & Power Division, STX Bldg., 448-2 Dogok 2-dong, Gangnam-gu, Seoul, Republic of Korea
[c*] Department of Mechanical Engineering, Hanyang University, 1271 Sa3-dong, Sangnok-gu, Ansan, Gyeonggi-do, Republic of Korea
E-mail: wskim@hanyang.ac.kr

ABSTRACT

In this study, the one-dimensional rate based model is developed for predicting the performance of the CO_2 absorber column using aqueous monoethanolamine (MEA) solution. To determine the concentration of each species and temperature distribution along the column height, mass and heat balance equations of vapor and liquid phase are coupled with chemical reactions in MEA-CO_2-H_2O system. The two-film model is applied to estimate the mass transfer in the vapour and liquid film. To calculate the enhancement factor, three types of reaction rate coefficient of the CO_2/aqueous MEA reaction are considered. The mathematical and reaction kinetics models used in this study are validated in the comparison of simulation results with experimental data given in the literature. The simulation results are in good agreement with the data in the literature. In addition, three types of reaction rate coefficient suggested by Hikita et al., Versteeg et al. and Aboudheir et al. are considered. The performance of CO_2 absorber column with respect to the reaction rate coefficients is compared with experimental data.

INTRODUCTION

CO_2 is regarded as a major greenhouse gas contributing to global warming. With growing concerns about the environmental impact of greenhouse gases, effective strategies such as Carbon Capture and Storage (CCS) are essentially required to reduce the CO_2 emission from a large CO_2 source.

The CO_2 capture technologies are usually divided into three main-categories: post-combustion, pre-combustion and oxy-fuel combustion. In the post-combustion technology, chemical absorption using a aqueous solution of chemical base is the most widely used process for the CO_2 capture in fossil fuel power plants. In chemical absorption, the most widely used solution is aqueous alkanolamine solutions. Examples of commonly used solutions are monoethanolamine (MEA),

NOMENCLATURE

a_t	[m^2/m^3]	Specific surface area
a_w	[m^2/m^3]	Effective interfacial area
C	[mol/m^3]	Concentration
C_p	[J/mol K]	Heat capacity
D	[m^2/s]	Diffusivity
E	[-]	Enhancement factor
H	[m^{3}kPa/mol]	Henry's law constant
ΔH_r	[J/mol]	Heat of reaction
ΔH_{vap}	[J/mol]	Heat of vaporization
h	[W/m^{2}K]	Specific interfacial heat transfer coefficient
K_{eq}	[mol^2/L^6],[mol/L^3]	Equilibrium constant
K_{ov}	[mol/m^{2}kPa s]	Overall mass transfer coefficient
k	[m/s]	Vapor and liquid side mass transfer coefficient
k_r	[m^3/mol s]	Reaction rate coefficient
N	[mol/m^{2}s]	Molar flux
P	[kPa]	Pressure
R	[J/mol K]	Gas constant
T	[K]	Temperature
t	[s]	Time
u	[m/s]	Velocity
z	[m]	Height

Greek symbols

α	[-]	CO_2 loading
ε	[m^3/m^3]	Holdup
ω	[-]	Wetted area ratio

Subscripts

i	Component
l	Liquid
v	Vapor

Superscripts

$*$	Interface value of variable
eq	Equlibrium
l	Liquid
v	Vapor

diethanolamine (DEA), methyldiethanolamine (MDEA) and etc. Among these solutions, MEA is the most widely used for CO_2 capture [1].

In the previous researches, various approaches at different levels of complexity were developed to predict the performance of CO_2 absorber column. Kenig et al. mentioned the different levels of complexity of various models [2]. The widely used approach for modeling and design of a reactive absorption process is the equilibrium stage model which subdivides the absorber column into several segments and assumes that the gas and liquid phase attain equilibrium at each stage [3]. In practice, equilibrium is hardly attained at each stage, because CO_2 absorption process is a rate-based-controlled phenomenon [4].

Therefore, in the present work, a rate-based model based on the two film theory is used to consider the resistance to mass transfer. The vapor-liquid equilibrium model is applied for predicting the mass transfer in vapor-liquid interface.

The works for the chemical reactions in MEA-CO_2-H_2O system were widely performed by Hikita et al. [5], Horng and Li [6], Crooks et al. [7], Versteeg et al. [8] and Aboudheir et al. [9]. In this study, the following chemical reactions are considered: ionization of water, dissociation of dissolved CO_2 through carbonic acid, dissociation of bicarbonate, carbamate reversion to bicarbonate, dissociation of protonated MEA and overall reaction of MEA and CO_2. Equilibrium constant proposed by Edwards et al. [10] and Kent et al. [11] are applied for the vapor-liquid equilibrium model.

Mass and heat balance equations for vapor and liquid phase are coupled with the interfacial mass transfer model and the vapor-liquid equilibrium model to determine the concentration distribution of each species and the temperature distribution along the height of column.

In this work, three types of reaction rate coefficient of the CO_2/aqueous MEA reaction are used in the rate based model. Then the rate based model used in this study is validated by comparing the simulation results with experimental results given in the literature.

MODELING

This section describes the rate based model of the absorber column for simulating the phenomena that happen in the MEA-CO_2-H_2O system.

Mass and heat balances

The partial differential equations (PDEs) are used to describe the time and spatial behaviour of concentration and temperature of the CO_2 absorption process in a plug flow reactor. Mass and heat balance equations of vapor and liquid phase are summarized below [12].

The species mass balance equations for the vapor and liquid phases are, respectively:

$$\varepsilon_v \frac{dC_i^V}{dt} = -u_v \frac{\partial C_i^V}{\partial z} - a_t N_i \tag{1}$$

$$\varepsilon_l \frac{dC_i^l}{dt} = -u_l \frac{\partial C_i^l}{\partial z} + a_t N_i \tag{2}$$

where ε_v and ε_l are the vapor and liquid holdup, C_i is the concentration of component i, u_v and u_l are the vapor and liquid velocities, a_t is the specific surface area and N_i is the mass flux of component i.

The heat balance equations for the vapor and liquid phases are, respectively:

$$\varepsilon_v \frac{dT_v}{dt} = -u_v \frac{\partial T_v}{\partial z} + \frac{a_t}{\sum\left(C_i C_{p,i}\right)_v} h_{v/l}(T_l - T_v) \tag{3}$$

$$\varepsilon_l \frac{dT_l}{dt} = -u_l \frac{\partial T_l}{\partial z} - \frac{a_t}{\sum\left(C_i C_{p,i}\right)_l} \{h_{v/l}(T_l - T_v) - \Delta H_r N_{CO_2} - \Delta H_{vap} N_{H_2O}\} \tag{4}$$

where T_v and T_l are the vapor and liquid temperature, $C_{p,i}$ is the specific heat capacity of component i, $h_{v/l}$ is the interfacial heat transfer coefficient, ΔH_r is the absorption heat of CO_2 and ΔH_{vap} is the vaporization heat of H_2O.

Interfacial mass transfer model

In this paper, the flux of CO_2, MEA and H_2O is defined as follows:

$$N_i = K_{ov,i}\left(P_i^{eq,*} - P_i^v\right)\omega \tag{5}$$

where $K_{ov,i}$ is the overall mass transfer coefficient, $P_i^{eq,*}$ is the equilibrium partial pressure of component i in the liquid phase and P_i^v is the partial pressure of component i in the vapor phase. The wetted area ratio ω is defined by

$$\omega = \frac{a_w}{a_t} \tag{6}$$

where a_w is the effective interfacial area of packing suggested by Seibert.

In this study, the mass transfer in the vapor-liquid interface is described by the two-film model. In two film theory, the overall mass transfer coefficient is defined in terms of the resistance to mass transfer in the vapor and liquid film. In case of MEA and H_2O, the resistance to mass transfer in the liquid film can be ignored since the MEA and H_2O concentrations are high in the liquid phase. Therefore, the overall mass transfer coefficient of MEA and H_2O is expressed by

$$K_{ov,i} = \frac{k_i^v}{RT_v} \tag{7}$$

where k_i^v is the vapor side mass transfer coefficient, R is the gas constant.

The overall mass transfer coefficient of CO_2 is given by

$$\frac{1}{K_{ov,CO_2}} = \frac{RT_v}{k_{CO_2}^v} + \frac{H_{CO_2}}{k_{CO_2}^l E_{CO_2}} \tag{8}$$

where H_{CO_2} is the Henry's law constant of CO_2, $k_{CO_2}^l$ is the

Table 1
Reaction rate coefficients of the CO_2/aqueous MEA reaction

Reference	Reaction rate coefficient $\left(\frac{\mathrm{m}^3}{\mathrm{mol\ s}}\right)$
Hikita et al. [5]	$k_r = 9.77 \times 10^7 exp\left(\frac{-4955}{T}\right)$
Versteeg et al. [8]	$k_r = 4.4 \times 10^8 exp\left(\frac{-5400}{T}\right)$
Aboudheir et al. [9]	$k_r = k_{r,MEA}C^*_{MEA} + k_{r,H_2O}C_{H_2O}$ $k_{r,MEA} = 4.61 \times 10^3 exp\left(\frac{-4412}{T}\right)$ $k_{r,H_2O} = 4.55 exp\left(\frac{-3287}{T}\right)$

Table 2
Equilibrium constants used in the VLE model [10] [11]

	a_1	a_2	a_3
$K_{eq,1}$, $(\mathrm{mol/L^3})^2$	-13445.90	-22.4773	140.93200
$K_{eq,2}$, $\mathrm{mol/L^3}$	-12092.10	-36.7816	235.48200
$K_{eq,3}$, $\mathrm{mol/L^3}$	-12431.70	-35.4819	220.06700
$K_{eq,4}$, $\mathrm{mol/L^3}$	-3090.83	0.0000	6.69425
$K_{eq,5}$, $\mathrm{mol/L^3}$	-5851.11	0.0000	-3.36360
$K_{eq} = exp\left(\frac{a_1}{T} + a_2 lnT + a_3\right)$			

mass transfer coefficient of liquid film and E_{CO_2} is the enhancement factor of CO_2 absorption. The correlations given by Onda et al. [13] for vapor and liquid side mass transfer coefficient are applied in this model.

The enhancement factor is defined as follows:

$$E_{CO_2} = \frac{\sqrt{k_{r,CO_2}C^*_{MEA}D_{CO_2}}}{k^l_{CO_2}} \tag{9}$$

where k_{r,CO_2} is the reaction rate coefficient for the reaction of CO_2 with the MEA solution, C^*_{MEA} is the free MEA concentration in liquid and D_{CO_2} is the diffusion coefficient of CO_2 in MEA solution.

Table 1 presents the reaction rate coefficients between CO_2 and MEA as suggested by Hikita et al. [5], Versteeg et al. [8] and Aboudheir et al. [9].

Vapor-liquid equilibrium model

To predict the mass transfer in the vapour-liquid interface, it is required to estimate the equilibrium pressure of CO_2 and the liquid concentration of all species present in the MEA solution. Therefore, the vapor-liquid equilibrium model is used for kinetic analysis. The chemical reactions considered are as follows:

Ionization of water:

$$2H_2O \overset{K_1}{\leftrightarrow} OH^- + H_3O^+ \tag{10}$$

Dissociation of dissolved CO_2 through carbonic acid:

$$CO_2 + 2H_2O \overset{K_2}{\leftrightarrow} HCO_3^- + H_3O^+ \tag{11}$$

Dissociation of bicarbonate:

$$HCO_3^- + H_2O \overset{K_3}{\leftrightarrow} CO_3^{2-} + H_3O^+ \tag{12}$$

Carbamate reversion to bicarbonate:

$$RNHCOO^- + H_2O \overset{K_4}{\leftrightarrow} RNH_2 + HCO_3^- \tag{13}$$

Dissociation of protonated MEA:

$$RNH_3^+ + H_2O \overset{K_5}{\leftrightarrow} RNH_2 + H_3O^+ \tag{14}$$

The liquid concentration of all species shown in the chemical reactions and their equilibrium partial pressure of species can be obtained by solving the following equations [9]:

MEA balance:

$$[RNH_2] + [RNH_3^+] + [RNHCOO^-] = [RNH_2]_0 \tag{15}$$

Carbon balance:

$$[CO_2] + [HCO_3^-] + [CO_3^{2-}] + [RNHCOO^-] = \alpha[RNH_2]_0 \tag{16}$$

Charge balance:

$$[RNH_3^+] + [H_3O^+] = [HCO_3^-] + [OH^-] + 2[CO_3^{2-}] + [RNHCOO^-] \tag{17}$$

Equilibrium constants:

$$K_1 = [OH^-][H_3O^+] \tag{18}$$

$$K_2 = \frac{[HCO_3^-][H_3O^+]}{[CO_2]} \tag{19}$$

$$K_3 = \frac{[CO_3^{2-}][H_3O^+]}{[HCO_3^-]} \tag{20}$$

$$K_4 = \frac{[RNH_2][HCO_3^-]}{[RNHCOO^-]} \tag{21}$$

$$K_5 = \frac{[RNH_2][H_3O^+]}{[RNH_3^+]} \tag{22}$$

The equilibrium pressure of each species:

$$P^{eq,*}_{CO_2} = H_{E,CO_2}C^*_{CO_2} \tag{23}$$

$$P^{eq,*}_i = x_i P_i \tag{24}$$

where α is the CO_2 loading, $C^*_{CO_2}$ is the free CO_2 concentration at equilibrium, x_i is the free MEA and H_2O mole fraction and

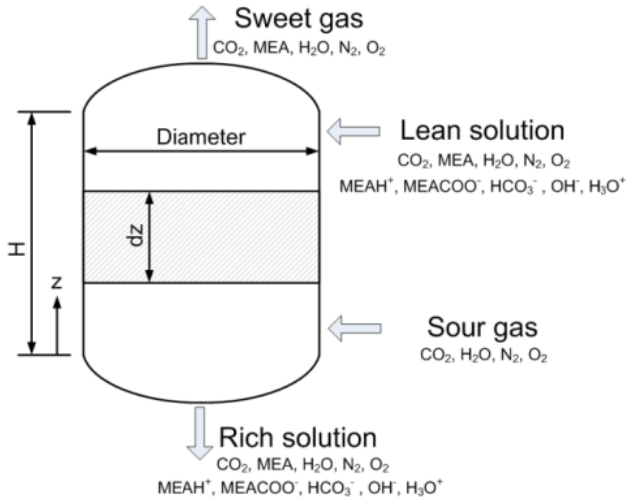

Figure 1 Schematic of CO_2 absorber column and control volume.

P_i is the partial pressure of MEA and H_2O. Table 2 shows the equilibrium constants used in this study.

MODEL VALIDATION

Figure 1 shows a schematic of CO_2 absorber column and a control volume used in the present study. It is assumed that the CO_2 absorber column is a packed column and vapor phase species are CO_2, MEA, H_2O, N_2 and O_2 while the liquid phase species are CO_2, MEA, H_2O, N_2, O_2, $MEAH^+$, HCO_3^-, OH^-, $MEACOO^-$ and H_3O^+. Flue gas enters at the bottom and flows upward through the packing while the CO_2 lean MEA solution is uniformly distributed at the top of the packing and flows downward.

Numerical method

The partial differential and algebraic equations were solved by in-house code using the Broyden's method. The spatial variables were discretized using the method of backward finite differences over a uniform grid of 200 elements.

Validation of vapor-liquid equilibrium model

To validate the equilibrium constants used in this study, the present results were compared with the experimental data given in Liu et al. [14]. The CO_2 loading was varied from 0 to 1 in a 2.5 M MEA solution at 313K. The concentration of each component was shown in Figure 2. The present results are in good agreement with those of Liu et al. [14]. With increasing CO_2 loading in the aqueous solution, MEA concentration is decreased. Otherwise the concentrations of main product, such as $[RNH_3^+]$, $[RNHCOO^-]$ and $[HCO_3^-]$, are increased because of the reaction between CO_2 and MEA. When the CO_2 loading is over 0.5, CO_2 absorption efficiency decreases, since the free MEA concentration is close to zero.

Validation of the rate-based model

The data from Dugas [15] is used to validate the rate based model in this study. Table 3 shows the absorber column and

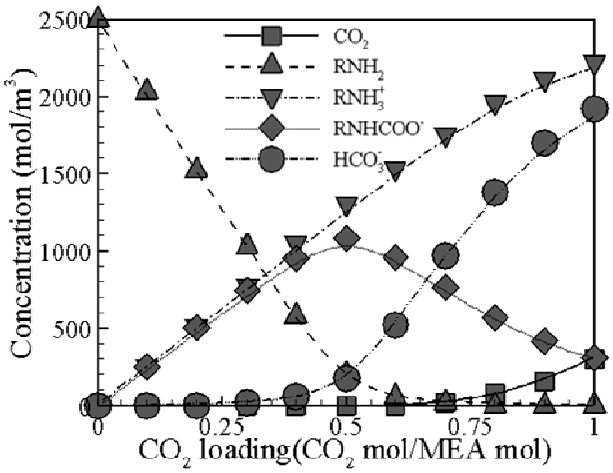

Figure 2 Liquid phase concentration in 2.5 M MEA solution with respect to CO_2 loading at 313 K.

Table 3
Absorber column and packing material data [15]

Absorber column	
Column inside diameter (m)	0.427
Column height (m)	11.1
Packing material data	
Packing type	IMTP-40
Height of packing (m)	6.1
Void fraction	0.98
Nominal packing size (m)	0.04
Specific surface area (m^2/m^3)	153

Table 4
Operating conditions of absorber column [15]

		Case25	Case41
Flue gas	Temperature(K)	328.12	325.50
	Flow rate(m^3/s)	679.23	678.96
	CO_2 fraction	0.173	0.171
Lean MEA	Temperature(K)	313.11	313.34
	Flow rate(m^3/s)	6.254	3.402
	CO_2 loading	0.278	0.235

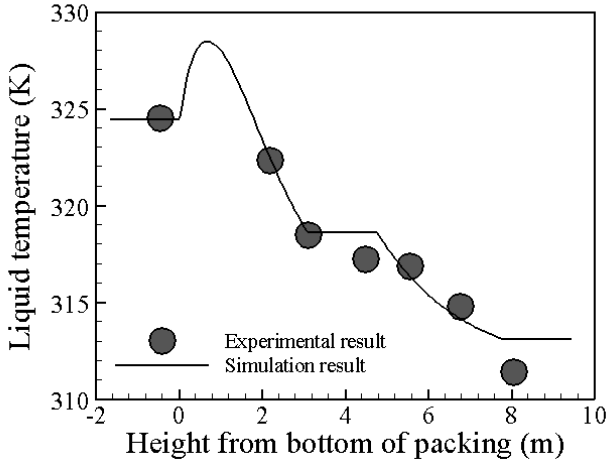

Figure 3 Comparison of the experiment [15] and simulation result for liquid temperature in Case 25.

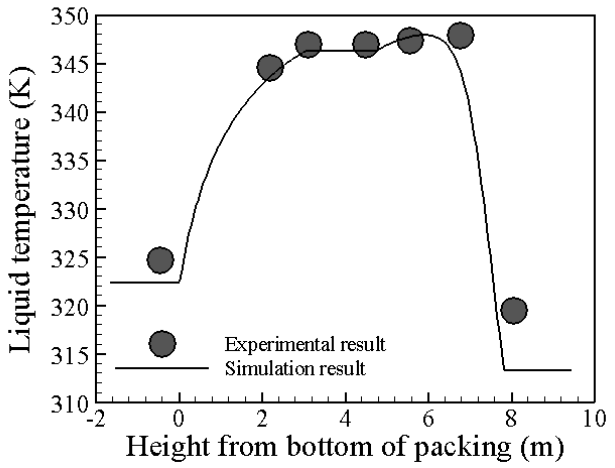

Figure 4 Comparison of the experiment [15] and simulation result for liquid temperature in Case 41.

Table 5
Comparison of the experiments [15] and simulation results

Case		Rich CO_2 loading (mol/mol)	CO_2 removal efficiency (%)
25	Exp.	0.386	93.0
	Sim.	0.398	92.4
41	Exp.	0.433	87.0
	Sim.	0.444	87.4

packing material data. The CO_2 absorber column of the pilot plant is a packed column with a total height of 11.1 m, a diameter of 0.427 m and total packing height of 6.1 m. The packing used in the absorber column is IMTP-40 with a void fraction of 0.98, a specific surface of 154 m^2/m^3 with a nominal packing size of 0.04 m.

Table 4 indicates the operating conditions of absorber column used in the validation of the present model. Among 48 experiments with various conditions performed by Dugas [15], two cases (Case 25 and 41) are selected to validate the rate based model for the absorber column. These selected cases represent relatively high and low liquid to vapor ratio, respectively.

The reaction rate coefficient of Aboudheir et al. [9] is used for validation of the rate based model. Figure 3 and 4 show the liquid temperature profiles of the experimental data [15] and the present simulation results for Case 25 and 41, respectively. The rich CO_2 loading and CO_2 removal efficiency are also validated by comparing the experimental and the simulation results as shown in Table 5. In the region that liquid temperature profile is uniform, it is assumed that the reaction between CO_2 and MEA solution is not occurred, since the packing does not exist. The liquid temperature profiles in the present study are in good agreement with the experimental results [15]. In addition, the rate based model used in this work can predict well rich CO_2 loading and CO_2 removal efficiency. In Case 25, the deviation of rich CO_2 loading and CO_2 removal efficiency is 0.4% and 3.3%, respectively. In Case 41, rich CO_2 loading and CO_2 removal efficiency show the deviation of 0.9% and 2.7%, respectively.

RESULTS AND DISCUSSIONS

In this work, the comparison of simulation results using various reaction rate coefficients suggested by Hikita et al. [5], Versteeg et al. [8] and Aboudheir et al. [9] with the pilot plant data from Dugas [15] is performed.

Case 25

Case 25 represents a relatively high liquid to vapor ratio. Figure 5 and 6 show the variations of the temperature and CO_2 loading in the liquid phase with respect to the reaction rate coefficients, respectively. As the MEA solution with lean CO_2 flows downward, the liquid temperature is gradually increased up to about 328 K because of the CO_2 absorption into MEA solution. The peak temperature is reached at the height of 0.4 m from bottom, since liquid flow rate is relatively high. Then the liquid temperature is decreased from 328 K to 325 K because of the vaporization of H_2O and the heat transfer between liquid and vapor phase. CO_2 loading is also increased up to about 0.4 since CO_2 is absorbed into MEA solution.

The simulation results using three types of reaction rate coefficient are compared with the experimental data as shown in Table 6. The CO_2 loading and the CO_2 removal efficiency using the reaction rate coefficients of Hikita et al. [5], Versteeg et al. [8] and Aboudheir et al. [9] are about 0.4 and 93~94%, respectively. This result shows that the rate based model using three types of reaction rate coefficient may well predict the behaviour of CO_2 absorber column in high liquid to vapor ratio.

Case 41

Case 41 shows a relatively low liquid to vapor ratio. Figure 7 and 8 indicate the variations of the temperature and CO_2 loading in the liquid phase with respect to the reaction rate coefficients, respectively. The results using the reaction rate

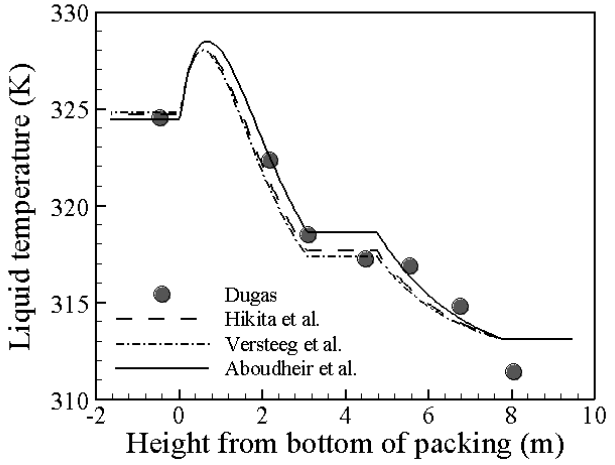

Figure 5 Variations of the temperature in the liquid phase with respect to the reaction rate coefficients for Case 25.

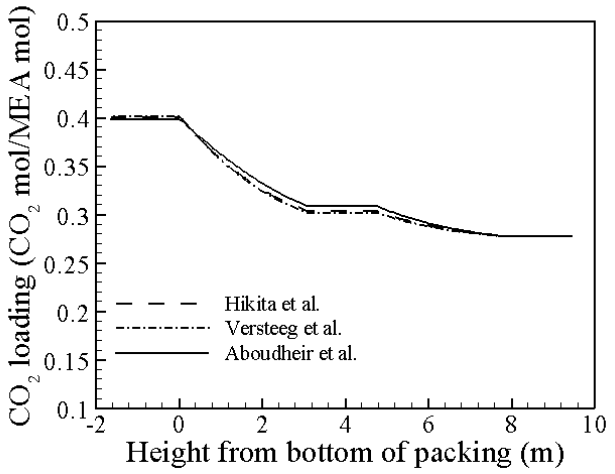

Figure 6 Variations of the CO_2 loading in the liquid phase with respect to the reaction rate coefficients for Case 25.

Table 6
Comparison of experiments and simulation results for Case 25

	Rich CO_2 loading (mol/mol)	CO_2 removal efficiency (%)
Dugas[15]	0.386	93.0
Hikita[5]	0.401	93.9
Versteeg[8]	0.402	94.7
Aboudheir[9]	0.398	92.4

coefficient of Hikita et al. [5], Versteeg et al. [8] and Aboudheir et al. [9] show the similar liquid temperature and the similar CO_2 loading profile. The liquid temperature is rapidly increased at the top of column and the peak temperature is shown to be about 348 K at the height of 6 m. Then the liquid temperature is sharply decreased.

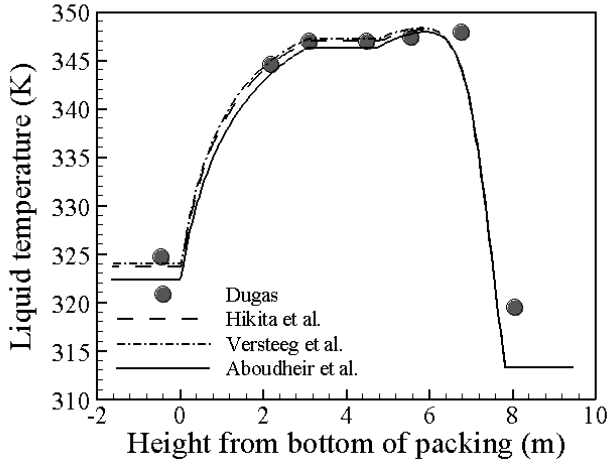

Figure 7 Variations of the temperature in the liquid phase with respect to the reaction rate coefficients for Case 41.

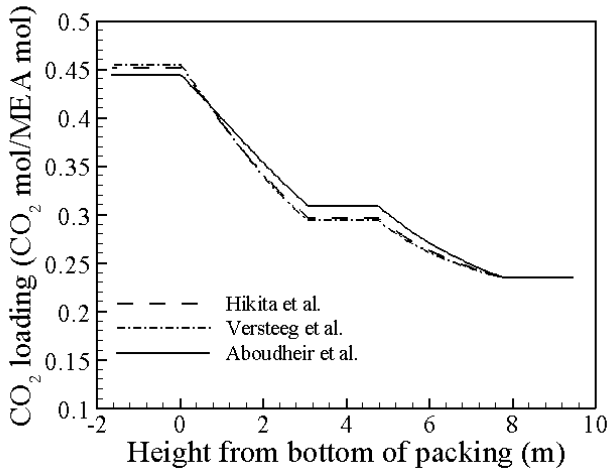

Figure 8 Variations of the CO_2 loading in the liquid phase with respect to the reaction rate coefficients for Case 41.

Table 7
Comparison of experiments and simulation results for Case 41

	Rich CO_2 loading (mol/mol)	CO_2 removal efficiency (%)
Dugas[15]	0.433	87.0
Hikita[5]	0.452	90.5
Versteeg[8]	0.455	91.7
Aboudheir[9]	0.444	87.4

It is due to the fact that the CO_2 absorption into MEA solution is mainly occurred at the top of absorber column. In addition, CO_2 loading is increased up to about 0.45 close to 0.5 at the bottom of absorber column. According to Eq. (5), CO_2 mass transfer at the interface is determined by the difference between the equilibrium pressure of liquid phase and the partial

pressure of vapor phase. Therefore, CO_2 mass transfer is decreased at the bottom of column and the position of peak temperature is shifted upward.

Table 7 indicates the comparison of the experimental data and the simulation results using three types of reaction rate coefficient. The liquid temperature profiles and the CO_2 loading profiles are shown to be similar and CO_2 removal efficiency obtained by using the reaction rate coefficient of Hikita et al. [5], Versteeg et al. [8] and Aboudheir et al. [9] is 90.5%, 91.7% and 87.4%, respectively. When the reaction rate coefficients of Hikita et al. [5] and Versteeg et al. [8] are applied to the present model, the CO_2 removal efficiency is 3~5% higher than that of Dugas [15]. However, the CO_2 removal efficiency obtained by using the reaction rate coefficient of Aboudheir et al. [9] is in good agreement with the experimental data. Therefore, the reaction rate coefficient of Aboudheir et al. [9] is more suitable than that of Hikita et al. [5] and Versteeg et al. [8] to predict the behaviour of CO_2 absorber column in relatively low liquid to vapor ratio.

CONCLUSION

In this work, the rate-based model is developed to analyze CO_2 absorption process under two operating conditions. Two cases represent relatively high and low liquid to vapor ratio, respectively. To validate the present model, the simulation results for two cases are compared with the pilot plant data and are in good agreement with the experimental data. In addition, the reaction rate coefficients suggested by Hikita et al. [5], Versteeg et al. [8] and Aboudheir et al. [9] are applied to the present model. Then the liquid temperature profile, CO_2 loading and CO_2 removal efficiency with respect to the reaction rate coefficients are compared with the experimental data.

In Case 25, the CO_2 loading and the CO_2 removal efficiency are respectively about 0.4 and 93~94%, when the reaction rate coefficients of Hikita et al. [5], Versteeg et al. [8] and Aboudheir et al. [9] are used. This result indicates that three types of reaction rate coefficient are appropriate to estimate the performance of CO_2 absorber column in high liquid to vapor ratio.

In Case 41, the liquid temperature profiles are shown to be similar for three types of reaction rate coefficient. The CO_2 removal efficiency obtained by using the reaction rate coefficient of Hikita et al. [5] and Versteeg et al. [8] is 3~5% higher than that of Dugas [15]. When the reaction rate coefficient of Aboudheir et al. [9] is employed in the present model, the results predict the CO_2 removal efficiency of 87.4%, which agrees well with the experimental data of Dugas[15] within the error of less than 1%. This result indicates that the reaction rate coefficient of Aboudheir et al. [9] is more suitable to analyze the CO_2 absorber column in low liquid to vapour ratio. It is shown in both cases that the rate-based model using the reaction rate coefficient suggested by Aboudheir et al. [9] is proper to predict the behaviour of CO_2 absorber column.

REFERENCES

[1] Akanksha, Pant K.K., and Sirvastava V.K., Carbon dioxide absorption into monoethanolamine in a continuous film contactor, *Chemical engineering Journal,*Vol. 133, 2007, pp. 229-237

[2] Kenig E.Y., Schneider R., and Górak A., Reactive absorption: optimal process design via optimal modelling. *Chemical Engineering Science,* Vol.56, 2001, pp.343–350

[3] Taylor R, Krishna R, Multicomponent mass transfer, *John Wiley and Sons, Inc.,* 1993

[4] Schneider, R., Kenig, E. Y., and Gorak, A., Dynamic modelling of reactive absorption with the maxwell–stefan approach, *Transactions of IChemE,*Vol. 77, 1999, pp. 633–638

[5] Hikita, H., Asai, S., Ishikawa, H. and Honda, M., The kinetics of reactions of carbon dioxide with monoethanolamine, diethanolamine and triethanolamine by a rapid mixing method, *Chemical Engineering Journal*, Vol. 13, 1977, pp. 7-12

[6] Horng, S. and Li, M., Kinetics of absorption of carbon dioxide into aqueous solutions of monoethanolamine + triethanolamine. *Industrial and Engineering Chemistry Research*, Vol. 41, 2002, pp. 257-266

[7] Crooks, J. E. and Donnellan, J. P., Kinetics and mechanism of the reaction between carbon dioxide and amines in aqueous solution, *Journal of Chemical Society of Perkin Transactions II*, 1989, pp. 331-333

[8] Versteeg, G. F., van Dijck, L. A. and van Swaaij, P. M., On the kinetics between CO_2 and alkanolamines both in aqueous an non-aqueous solutions, An overview. *Chemical Engineering Communications*, Vol. 144, 1996, pp. 113-158

[9] Aboudheir, A., Tontiwachwuthikul, P., Chakma, A. and Idem, R., Kinetics of the reactive absorption of carbon dioxide in high CO_2-loaded, concentrated aqueous monoethanolamine solutions, *Chemical Engineering Science*, Vol. 58, 2003, pp. 5195-5210

[10] Edwards, J. T., Maurer, G., Nuwman, J. and Prausnitz, J. M., Vapor-liquid equilibria in multicomponent aqueous solutions of volatile weak electrolytes, *A.I.CH.E Journal*, Vol. 24, No. 6, 1978, pp. 966-976

[11] Kent, R. L. and Eisenberg, B., Better data for amine treating, *Hydrocarbon Processing*, February, 1976, pp. 87-90

[12] Kvamsdal, H. M., Jkobsen, J. P. and Hoff, K. A., Dynamic modeling and simulation of a CO_2 absorber column for post-combustion CO_2 capture, *Chemical Engineering and Processing*, Vol. 48, 2009, pp. 135-144

[13] Onda, K., Takeuchi, H. and Okumuto, Y., Mass transfer coefficients between gas and liquid phases in packed columns, *Journal of Chemical Engineering Japan*, Vol. 1, 1968, pp. 56-62

[14] Liu Y., Zhang L., and Watanasiri S., Representing Vapor-liquid equilibrium for an aqueous MEA-CO_2 system using the electrolyte nonrandom-two-liquid model, *Industrial Engineering Chemical Research*, Vol. 38, 1999, pp. 2080-2090

[15] Dugas, R. E., Pilot plant study of carbon dioxide capture by aqueous monoethanolamine, Master Thesis, The University of Texas at Austin, Chemical Engineering, 2006